J Wood Sci (2006)
DOI 10.1007/s10086-005-0753-4

ORIGINAL ARTICLE

Jonas Danvind · Mats Ekevad

Local water vapor diffusion coefficient when drying Norway spruce sapwood

Received: April 19, 2005 / Accepted: July 20, 2005

Abstract In this article, a one-dimensional and a two-dimensional approach to the evaluation of local diffusion coefficients for Norway spruce sapwood from measured moisture content (MC) values are presented. A studied wood sample was dried from the initial green condition to about 15% mean MC, but here only the diffusive part of the drying process between approximately 25% and 15% mean MC was treated. Measured local MC values were based on nondestructive X-ray computed tomography data. Finite element calculations were performed with two alternative diffusion coefficients to test the appropriateness of the diffusion coefficients that were evaluated from the measured MC values. The evaluated diffusion coefficients show interesting dependence on MC and distance from the evaporation surface. The advantage of using the methods presented is that the diffusion coefficient is calculated on a local level without having to define a function for the diffusion coefficient's dependency on other parameters.

Key words Wood · FEM · Drying · Diffusion coefficient · Computed tomography

Introduction

When physically describing the drying behavior of wood, the drying process can be divided into the capillary part and the diffusion part. In the capillary part, the moisture content (mass of water/mass of dry wood; MC) is high and there is free water present in the voids of the wood fibers. When the MC is lower and there is moisture only bound in the cell walls of the fibers, then the moisture flux is driven by diffusion. Internal stresses are induced in the diffusion part of the drying process due to anisotropic shrinkage, which may cause checking and drying distortions that reduce the quality of the timber. Large MC gradients during the diffusive process give a fast drying process but cause large stresses. It is of importance to understand the drying behavior of wood in order to avoid quality degradation due to drying. One way to do this is through simulation.

Simulations of the wood drying process using three-dimensional (3D) finite element method (FEM) can provide detailed and realistic information about the local MC, local stress, and global deformation history. 3D FEM calculations require, among other material data, diffusion coefficients that are valid locally throughout the material. The objective of this work is to determine local diffusion coefficients using nondestructive measurements and numerical methods.

Alternative approaches to the evaluation of local diffusion coefficients for Norway spruce sapwood are presented based on experiment. A clearwood sample (Fig. 1) was dried from the initial green condition to about 15% mean MC (mean value for the wood sample in question), but here only the diffusive part of the drying process between approximately 25% and 15% mean MC was treated. The measured local MC values were based on nondestructive X-ray computed tomography (CT) data.

Several authors (Hukka,[1] Hukka and Oksanen,[2] Liu et al.,[3] Rosenkilde and Arfvidsson[4]) have found that the diffusion coefficient for a certain wood sample is not constant, but is dependent on MC in addition to the dependence on temperature. The diffusion coefficients obtained are global mean values for a wood sample of a certain size.

The CT method used here to measure local interior two-dimensional (2D) densities and MCs of the wood sample is described by Lindgren,[5] Danvind and Moren,[6] and Wiberg.[7] The advantage of using the methods presented in this article is that the diffusion coefficient is calculated on a local level

J. Danvind · M. Ekevad (✉)
Division of Wood Technology, Skellefteå Campus, Luleå University of Technology, Skeria 3, Skellefteå SE-931 87, Sweden
Tel. +46-910-585300; Fax +46-910-585399
e-mail: mats.ekevad@ltu.se

J. Danvind
Valutec AB, Skellefteå SE-931 27, Sweden

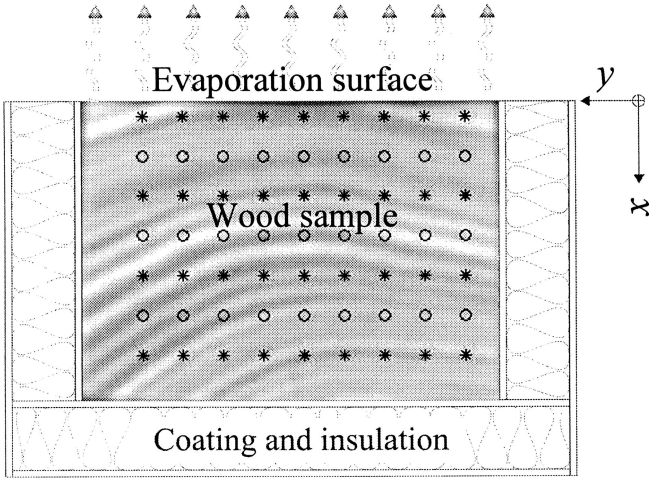

Fig. 1. Wood sample. *Asterisks* and *circles* denote center points of cells

without having to define a function for the diffusion coefficient's dependencies on other parameters such as MC. The possibility of using CT data to determine local properties in wood other than moisture properties, such as spiral grain angles, is demonstrated by Ekevad[8] and Sepulveda et al.[9]

Theory

Isothermal conditions are considered, and a Cartesian coordinate system and a referential (Lagrangian) viewpoint are adopted in order to deal with the shrinkage of the material. Thus, the coordinates x, y, and z denote the coordinates of a material point in the green condition, and all lengths, areas, and volumes are values in this green state and remain constant during the drying process. In the first approach to determining the diffusion coefficient D, the moisture flux is assumed to be one dimensional (1D) in the radial direction (x) and a modified Fick's first law is stated as

$$g = -D\frac{du}{dx}. \tag{1}$$

where $g = g(x, t)$ is the mass flux in the positive x direction per unit area at position x at time t, $u = u(x, t)$ is the MC at x and t. u is used as the driving potential in the modified Fick's first law (Eq. 1) instead of using the moisture concentration $w = u\,\rho_0$, where $\rho_0 = \rho_0(x)$ is the basic density of wood (dry mass of wood per green volume). It was found experimentally that u is a better way to express the amount of moisture in our case where ρ_0 varied in space (Fig. 2). This was confirmed in our experiments, because it was found that a gradient $dw/dx \neq 0$ could exist without creating a mass flux, due to local variations of ρ_0. In that case, $dw/dx \neq 0$ due to a gradient $d\rho_0/dx \neq 0$ but $du/dx = 0$. Physically it can be reasoned that u is a better measure of MC than w when it comes to bound water diffusion because water molecules are attracted to wood molecules and not to a specific volume. Mass conservation and Eq. 1 give

$$\dot{u} = \frac{1}{\rho_0}\frac{d}{dx}\left(D\frac{du}{dx}\right) \tag{2}$$

which is a modified Fick's second law. The general boundary conditions to be used with Eqs. 1 and 2 are specified values of u (essential conditions) or g (natural conditions) or

$$g = \beta(u - u_\infty) \tag{3}$$

(convective conditions or mixed conditions) on all or parts of the boundaries. Here the convective condition is used for the evaporation surface and the natural condition $g = 0$ for all the other surfaces. The initial condition is $u = u_0(x, t_0)$ at the starting time t_0. β is the mass transfer coefficient for the moisture vaporization into the surrounding air on the boundary surface, and u_∞ is the equilibrium MC for wood under ambient air conditions.

The equations for 2D mass flux in the x and y directions are a modified Fick's first law for an orthotropic material,

$$\boldsymbol{g} = \left(g_x, g_y\right)^T = -\boldsymbol{D}\,\mathrm{grad}(u) = -\boldsymbol{D}\left(\frac{\partial u}{\partial x}, \frac{\partial u}{\partial y}\right)^T \tag{4}$$

where

$$\boldsymbol{D} = \begin{bmatrix} D_{xx} & D_{xy} \\ D_{yx} & D_{yy} \end{bmatrix} \tag{5}$$

is the symmetric diffusion coefficient matrix. Here it is assumed that radial and tangential directions coincide with the x and y directions, respectively (Fig. 1). Mass conservation and Eq. 4 give

$$\dot{u} = \frac{1}{\rho_0}\mathrm{div}\left[\boldsymbol{D}\,\mathrm{grad}(u)\right] \tag{6}$$

or expanded

$$\rho_0\frac{\partial u}{\partial t} = \frac{\partial}{\partial x}\left(D_{xx}\frac{\partial u}{\partial x} + D_{xy}\frac{\partial u}{\partial y}\right) + \frac{\partial}{\partial y}\left(D_{yx}\frac{\partial u}{\partial x} + D_{yy}\frac{\partial u}{\partial y}\right) \tag{7}$$

which is a modified Fick's second law. The boundary conditions are specified values of u or $\boldsymbol{g}$ or convective conditions (Eq. 3). The initial condition is $u = u_0(x, y, t_0)$.

Materials and methods

A wood sample made of clear sapwood of Norway spruce (*Picea abies*) with the green dimensions of 31, 42, and 205 mm in the x (radial), y (tangential), and z (longitudinal) directions, respectively, was dried in this study. Five surfaces of the sample were coated using polyurethane glue (Cascol 1809, Casco) and aluminum foil (Fig. 1). The coated

surfaces were also thermally insulated using Styrofoam. Three temperature sensors were placed within the sample at 1, 11, and 21 mm depths from the surface, but in different positions in the longitudinal direction. One additional sensor was placed on the surface. During drying, the humidity, temperature, and speed of the circulating air was approximately constant at 43% relative humidity, 50°C, and 4 m/s, respectively. A Siemens Somatom AR.T. X-ray CT scanner was used to capture a density image in the tangential–radial plane of the interior at a constant longitudinal position every 10 min during drying.

Evaluation of D from the CT data, 1D method

$u(x, t)$ values for small volumes ($0.14 \times 0.14 \times 5\,\text{mm}^3$) in 3D space (voxel values) were measured with CT (see Danvind and Morén[6] for a description of the method). In order to reduce spread and increase accuracy, mean MCs $u(x_i, t_j)$ for seven discrete volumes along the x axis with center positions at $x_i = 2.0$, 5.9, 9.8, 13.7, 17.6, 21.6, and 25.5 mm for $i =$ 1 to 7 were evaluated. A value of u at $x_8 = 29.2$ mm was set equal to the value of u at $x = x_7$. $x_0 = 0$ was the surface position, and $x_9 = 31.0$ mm denoted the inner, insulated boundary. u values were measured at discrete time points, t_k, between $t_0 = 0$ h and $t_{200} = 100$ h with a time step of 0.5 h, except between $t = 83$ h and $t = 95$ h and between $t = 42.5$ h and $t = 44$ h due to malfunction of the equipment. Denoting d/dx with a prime, using mass conservation and a central difference scheme we get the mass flux gradient,

$$g_i'^k = -\rho_{0i}\dot{u}_i^k = -\rho_{0i}\frac{\left(u_i^{k+1} - u_i^{k-1}\right)}{\left(t_{k+1} - t_{k-1}\right)} \tag{8}$$

where the subindex i denotes the position $x_i = 2.0$, 5.9 . . . 29.2 mm for $i = 1$ to 8 and superindex k denotes the time step $t_k = 0$, 0.5, 1.0 . . . h for $k = 1$ to 199. Integration of Eq. 8 gives the surface mass flux

$$g_{\text{surf}}^k = g\left(0, t_k\right) = -\int_0^l g' dx = -\sum_{i=1}^{8} g_i'^k \Delta x_i \tag{9}$$

where $\Delta x_i = x_{i+1} - x_i$ is the length in the x direction of the volume associated with each value u_i. The mass flux at position i is

$$g_i^k = g\left(x_i, t_k\right) = g_{\text{surf}}^k + \int_0^x g'^k dx = g_{\text{surf}}^k + \sum_{l=1}^{i} g_l'^k \Delta x_l \tag{10}$$

where Δx_l is the length in the x direction of each of the volumes that has x coordinates lower than x_i. Now Eq. 1 with a central difference scheme gives

$$D_i^k = -\frac{g_i^k}{u_i'^k} = -\frac{g_i^k\left(x_{i+1} - x_{i-1}\right)}{\left(u_{i+1}^k - u_{i-1}^k\right)} \tag{11}$$

The mass transfer coefficient β is evaluated from Eq. 3 as

$$\beta^k = \frac{g_{\text{surf}}^k}{\left(u_{\text{surf}}^k - u_\infty^k\right)} \tag{12}$$

where u_{surf}^k is evaluated by a parabolic extrapolation to the surface using the three u_i values that are closest to the evaporation surface.

Evaluation of D from the CT data, 2D method

Mean $u(x, y, t)$ values for cells, $4.1 \times 4.1 \times 5\,\text{mm}^3$, in 3D space are evaluated from the CT data. The total mass flux, g_{surf}^k, transferred from the sample at time $t = t^k$ is calculated by using the total mass decrease, the time step $\Delta t^k = t^{k+1} - t^{k-1}$ and the area of the convective surface, A_{surf}. The mass flux is

$$g_{\text{surf}}^k = \frac{\sum_{i=1}^{M}\sum_{j=1}^{N}\left(m_{i,j}^{k+1} - m_{i,j}^{k-1}\right)}{\Delta t^k \cdot A_{\text{surf}}} \tag{13}$$

where subindices i and j denote the positions in the x and y directions, respectively. $M = 7$ and $N = 9$ are the number of cells in the x and y directions, respectively (Fig. 1), and m is mass.

The mass transfer coefficient, β^k, at time $t = t^k$ is calculated as

$$\beta^k = \frac{g_{\text{surf}}^k A_{\text{surf}}}{\sum_{j=1}^{N}\left(u_\infty - u_{\text{surf,j}}^k\right)A_{\text{surf,j}}} \tag{14}$$

where $u_{\text{surf},j}^k$ is the MC at time $t = t^k$ for the surface of a cell adjacent to the evaporation surface with $y = y_j$. $u_{\text{surf},j}^k$ is linearly extrapolated from the MCs of the two cells next to the surface. $A_{\text{surf},j}$ is the evaporation surface area of the cell at $y = y_j$. The modified Fick's first law of diffusion (Eq. 4) is used for the mass flux of the interior cell's boundary surfaces. In the first iteration of an iterative scheme, the coupling term, D_{xy} in Eq. 5, is set equal to zero. For a cell on the evaporation surface at position $(i, j) = (\text{surf}, j)$, surface mass transfer is assumed to govern the mass flux, which is calculated using β^k from Eq. 14. The modified Fick's second law (Eq. 7) is used for mass balances in cells, and the spatial derivatives of D are assumed to be zero in a cell. Based on these assumptions, Eq. 7 can be stated in numerical form as:

$$\begin{aligned}
\rho_0\frac{u_{ij}^{k+1} - u_{ij}^{k-1}}{t^{k+1} - t^{k-1}} &= \frac{1}{\Delta x}\left[D_{x,i-0.5,j}^k \cdot \frac{u_{i-1,j}^k - u_{i,j}^k}{x_{i-1,j} - x_{i,j}} - D_{x,i+0.5,j}^k \cdot \frac{u_{i,j}^k - u_{i+1,j}^k}{x_{i,j} - x_{i+1,j}}\right] \\
&+ \frac{1}{\Delta y}\left[D_{y,i,j-0.5}^k \cdot \frac{u_{i,j-1}^k - u_{i,j}^k}{y_{i,j-1} - y_{i,j}} - D_{y,i,j+0.5}^k \cdot \frac{u_{i,j}^k - u_{i,j+1}^k}{y_{i,j} - y_{i,j+1}}\right] \\
&= \begin{bmatrix} x_{i-1,j} - x_{i,j} = x_{i,j} - x_{i+1,j} = \Delta x; \\ y_{i,j-1} - y_{i,j} = y_{i,j} - y_{i,j+1} = \Delta y; \\ D_{x,i-0.5,j}^k = D_{x,i+0.5,j}^k = D_{x,i,j}^k; \\ D_{y,i,j-0.5}^k = D_{y,i,j+0.5}^k = D_{y,i,j}^k \end{bmatrix} = D_{x,i,j}^k \cdot \frac{1}{\Delta x^2} \\
&\cdot\left[u_{i-1,j}^k - 2u_{i,j}^k + u_{i+1,j}^k\right] + D_{y,i,j}^k \cdot \frac{1}{\Delta y^2} \cdot \left[u_{i,j-1}^k - 2u_{i,j}^k + u_{i,j+1}^k\right]
\end{aligned} \tag{15}$$

In Eq. 15 it is assumed that all elements have the same size, Δx, and Δy. From the CT experiments, all parameters except $D_{x,i,j}$ and $D_{y,i,j}$ can be achieved for each cell of 30×30 voxels in the CT image. Hence, there is one equation (Eq. 15) and two unknowns for each cell; thus, the equation system for all elements is underdetermined. By setting $D_{x,i,j}$ and $D_{y,i,j}$ equal in adjacent cells, in this case 2×6 cells (8.1×24.3 mm), the number of unknowns for the equation system is reduced, and thereby an overestimated system is achieved which is solved in a least-squares sense using standard Matlab[10] routines. By moving the position of the 2×6 cells and repeating the calculation procedure 12 times, once for each movement of the cells, 12 sets of $D_{x,i,j}$ and $D_{y,i,j}$ are achieved in each cell. The median values of the 12 solution sets are then taken as estimated solutions of $D_{x,i,j}$ and $D_{y,i,j}$ in each cell.

In a second iteration using $u_{i,j}$, $D_{x,i,j}$, and $D_{y,i,j}$, the mass fluxes, $g_{x,i,j}$ and $g_{y,i,j}$, are calculated using a numerical form of Eq. 4. $g_{x,i,j}$ and $g_{y,i,j}$ are used to recalculate the diffusion coefficients, including the coupling term, D_{xy}. This procedure gives two equations and three unknowns, D_{xx}, D_{yy}, and D_{xy}, per cell; i.e., when setting up a matrix system of equations for all cells, an underdetermined system is obtained. This time the number of unknowns is reduced by setting D_{xx}, D_{yy}, and D_{xy} constant in 2×2 cells and by solving the overdetermined system in a least-squares sense. As before, by moving the position of the 2×2 cells and by solving the system four times, four sets of diffusion coefficients per cell are achieved in each cell, and the median values are chosen as solutions. Using the coupled diffusion coefficients, local mass fluxes can be derived, and the procedure of deriving diffusion coefficients can be iterated until values stabilized. Here, only the first and second iterations have been done. In this study, the diffusion in the radial direction (x) was to be studied. Therefore, diffusion coefficients in the horizontal direction (y) of the CT image are not presented.

FEM calculation

ABAQUS[11] was used with a 3D isothermal and isotropic diffusion model as a solver of the diffusion equation (Eq. 6). As boundary conditions, we had zero mass flux on five surfaces and convection on the evaporation surface (Fig. 1). The initial condition $u(x, t_0)$ at $t_0 = 30.1$ h was taken from the measured data. Based on experimental findings shown below, two alternatives for D were used. As the first alternative $D = D(u)$ was adapted, and as a second alternative $D = D(u, x)$ was used. The measured values of $\beta(u)$ were used during the FEM calculations.

Results

All results shown in this article relate to the diffusion part of the total drying process and hence use a time scale that starts at time 30.1 h. The temperature differences between three internal positions in the test sample and in the air were <0.8°C during the test. $\rho_0(x)$ is shown in Fig. 2, $u(t)$ for different x values is shown in Fig. 3, and $u(x)$ for different times in Fig. 4. $D(u)$ for the 1D method is shown in Fig. 5 for $x \le 13.7$ mm and $\beta(u)$ is shown in Fig. 6. For the 2D method, $D(u)$ is shown in Fig. 7 and $\beta(u)$ in Fig. 6. The objective in the FEM calculations was to find D values that gave $u(x)$ good correlation to the experimental result at the final time $t = 99$ h. The agreement between experiment and calculation was then checked at an intermediate time $t = 65$ h. The FEM simulation using the first alternative $D = D(u)$ according to Fig. 8a gives an agreement with the CT measurements according to Fig. 4a. The second alternative $D = D(u,x)$ according to Fig. 8b has an agreement according to Fig. 4b.

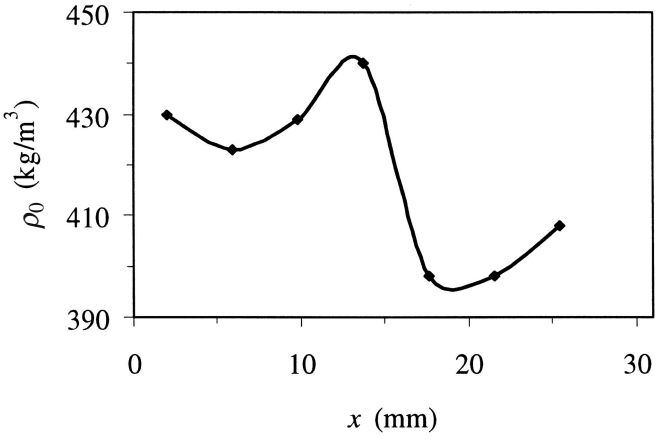

Fig. 2. Measured basic density $\rho_0(x)$

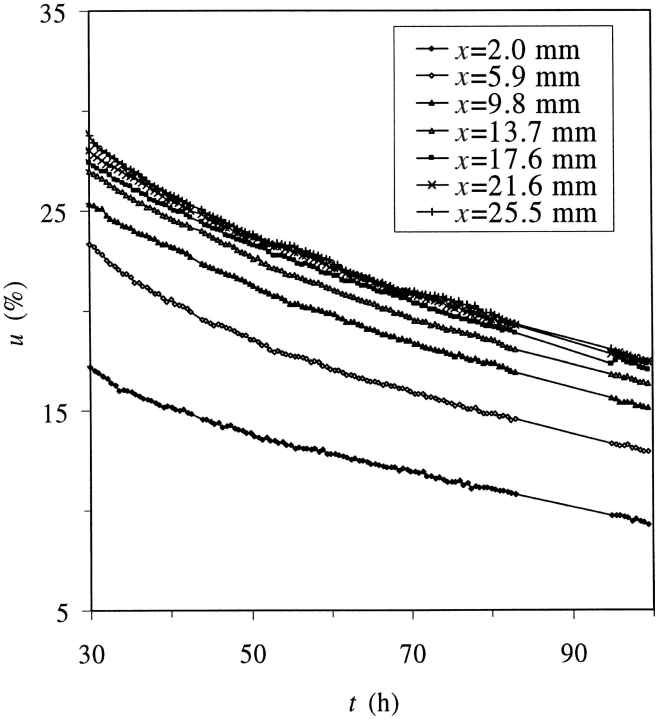

Fig. 3. Measured moisture content $u(t)$ for different x values in consecutive order from the lowest curve with the lowest x value

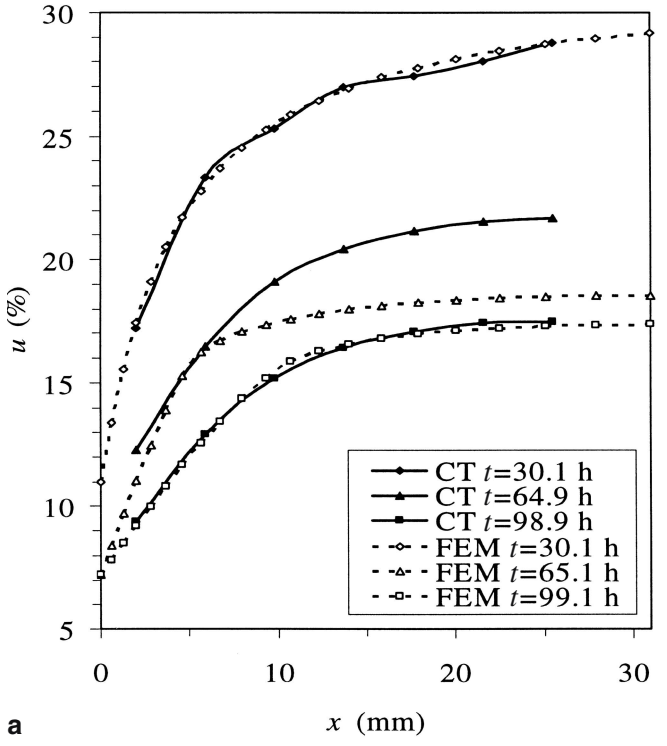

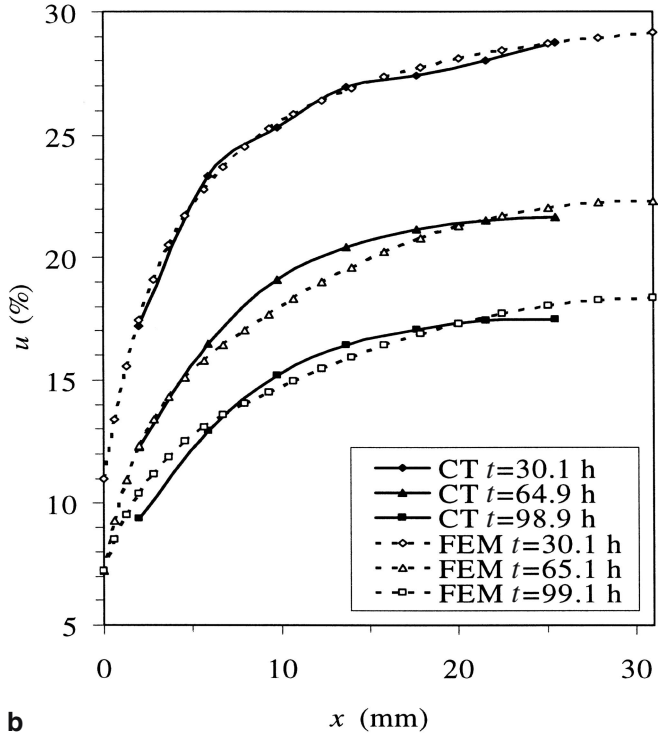

Fig. 4a,b. Moisture content $u(x)$ at different times t measured with computed tomography and calculated with finite element method (FEM). **a** FEM approach $D = D(u)$. **b** FEM approach $D = D(u, x)$

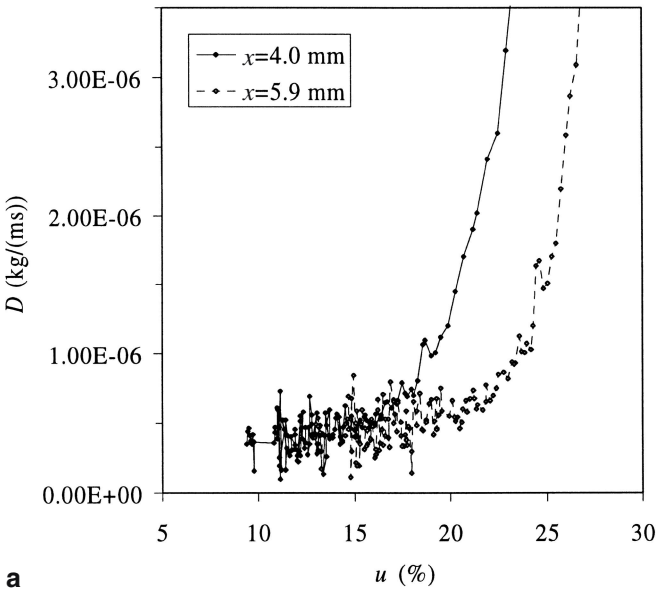

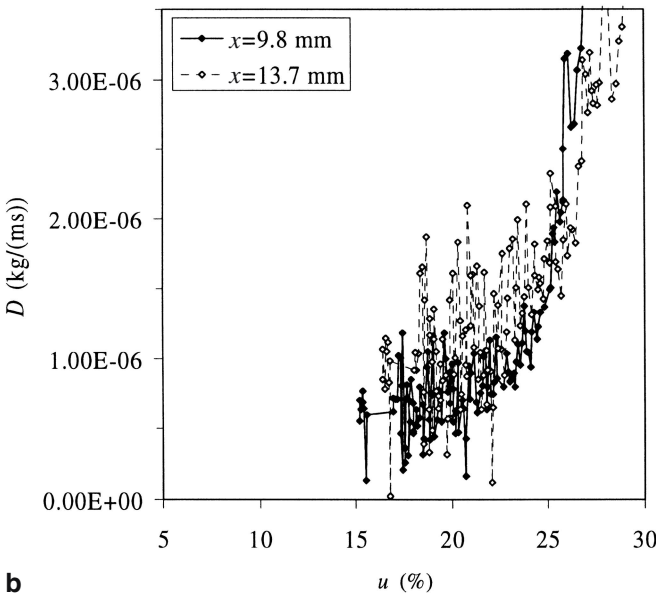

Fig. 5a,b. $D(u)$ evaluated with the one-dimensional (1D) method for different x values. **a** x = 4.0 and 5.9 mm. **b** x = 9.8 and 13.7 mm

The initial conditions u_0 at t_0 = 30.1 h for the FEM simulations are the same for both alternatives.

Discussion

For the 1D method, D shows a rather clear dependence on u and x as is seen from Fig. 5. The curves for x = 5.9, 9.8, and 13.7 mm agree well (Fig. 5) but the curve for x = 4.0 mm is translated to the left and downward compared with the other curves. The curve for x = 17.6 mm (not shown) agrees quite well with the curves for x = 5.9, 9.8, and 13.7 mm, but shows more spread. The curves for x = 21.6 and 25.5 mm

(not shown) show even more spread, but they seem to agree with the curves for x = 5.9, 9.8, 13.7, and 17.6 mm. Thus, there is a unique curve for x = 4.0 mm, and all of the rest of the curves at the other x values seem to agree reasonably well. The reason for the large spread of D for large x values is probably the decreasing MC gradient and the decreasing mass flux with depth (x), which make the numerical errors large (Eq. 11). The overall conclusion is that the diffusion coefficient is a function of MC and depth, $D = D(u,x)$. The dependence on u is especially large in the interval where $16\% < u < 30\%$, while for $u < 16\%$, D seems rather constant.

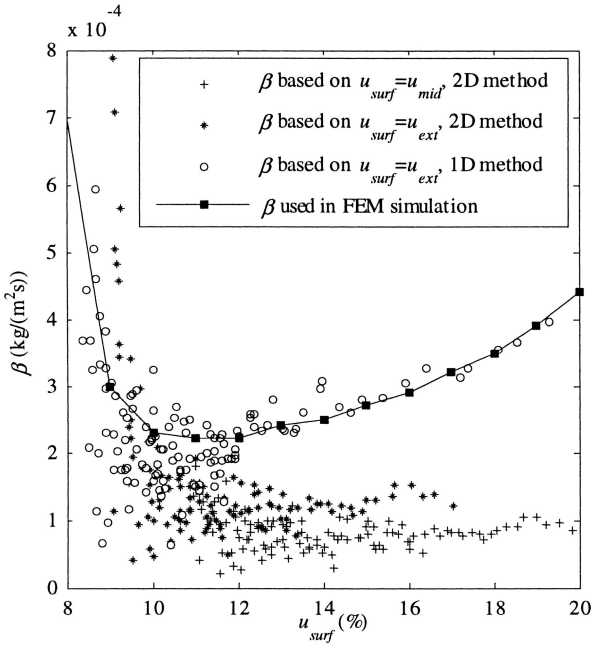

Fig. 6. $\beta(u)$ evaluated with the 1D and 2D methods with alternative surface moisture contents. u_{ext}, linear extrapolation from two adjacent u values or parabolic extrapolation from three adjacent u values; u_{mid}, mean value of the surface cell; i.e., $u_{mid} = u(x_{i=1}, t^k)$

The dependence on the distance from surface x is only significant when $x < 5$ mm, i.e., near the surface. β shows more spread at lower mean MC due to smaller $u_{surf} - u_\infty$ than at higher mean MC (Fig. 6).

For the 2D method, only D_x values are presented. This is due to large spread in D_y, probably caused by the one-directional drying resulting in almost constant values of u in the y direction, which strongly influenced the derivation of D_y. D_x values (Fig. 7) are similar to the results from the 1D method, but the results have less spread. A reason for the lower spread is probably the calculation method in which the median values of several solution sets are taken as D. β values for the 2D method are lower than for the 1D method (Fig. 6). This is due to the different choices of u_{surf}.

When trying to reproduce the original, measured $u(x)$ values at t = 99.1 h with the FEM calculation, the second alternative with $D = D(u, x)$ is best (Fig. 4b). This shows the validity of the experimentally derived D values and the dependence of D on distance to the evaporation surface. The first alternative with $D = D(u)$ gave good correlation at t = 99.1 h but poor correlation at t = 65.1 h (Fig. 4a).

In Fig. 8b, evaluations of D from Hukka[1] and Rosenkilde and Arfvidson[4] are compared with our values used for FEM calculations. Their values and ours agree quite well, at least for $u < 15\%$. The discrepancy in D for $u > 20\%$ between our values and theirs could be due to differences in wood material (Hukka[1] used Norway spruce heartwood and Rosenkilde and Arfwidson[4] used Scots pine sapwood) and differences in evaluation methods. Hukka[1] assumed that $D(u)$ is an exponential function and Rosenkilde and Arfvidson[4] used another type of curve-fitting method. The rate of the mean MC for a wood sample is essentially controlled by β and not D when u is high, and vice versa. However, an appropriate $D(u)$ description is important for realistic local $u(x)$ values.

The dependence on depth can be a dependence not on depth itself but via some other parameter (not measured

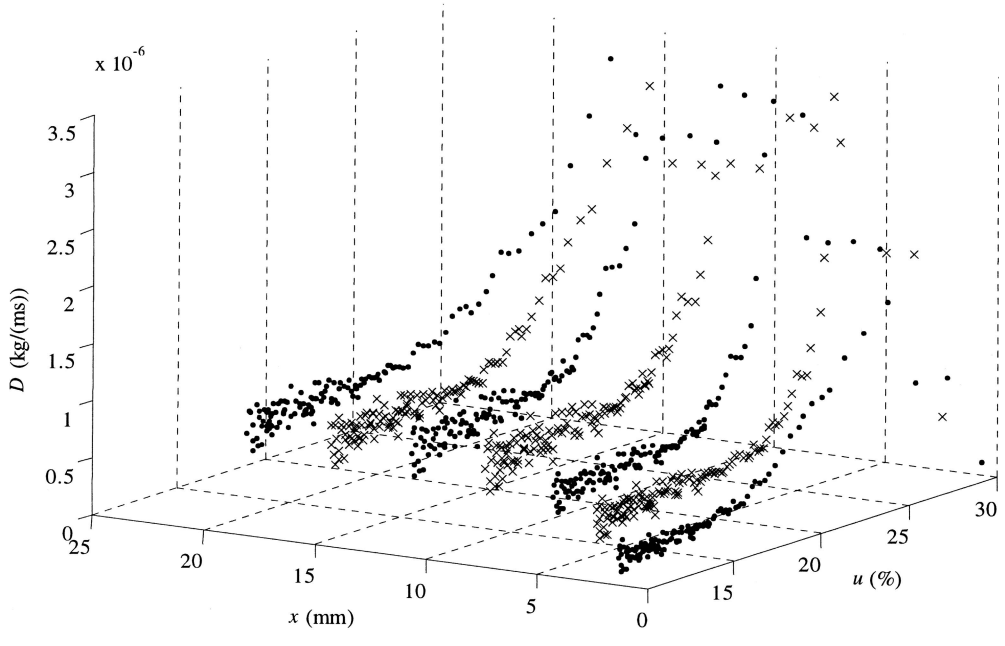

Fig. 7. Diffusion coefficient $D(u,x)$ evaluated with the 2D method. x = 2.0, 5.9, 9.8, 13.7, 17.6, 21.6, 25.5 mm shown as alternating series of *dots* and *crosses*

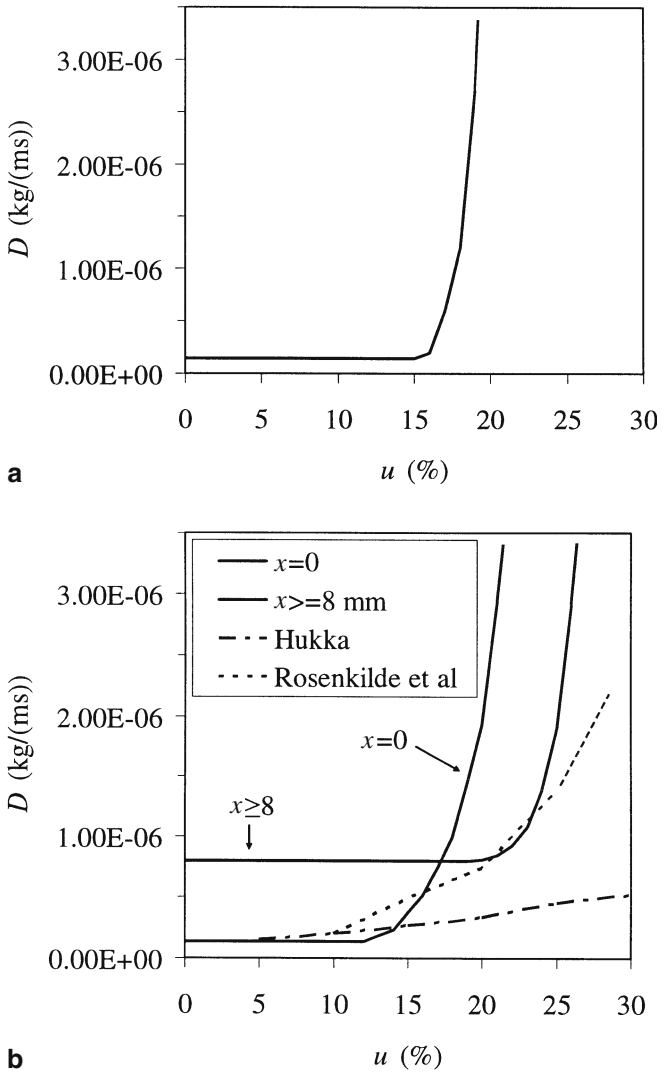

Fig. 8. **a** $D(u)$ used in the first approach of FEM calculations. **b** $D(u, x)$ used in the second approach of FEM calculations. Linear interpolation of D for $0 < x < 8$ mm using the curves for $x = 0$ and $x = 8$ mm. Comparison values of Hukkas[1] values are for Norway spruce heartwood, those of Rosenkilde and Arfvidssons[4] are for Scots pine sapwood

here), which itself is a function of depth. Such a parameter is stress, because there are probably large stresses near the surface. Also, $\dot{u}$ is a function of depth because the material near the surface has a faster changing moisture situation than the material far away from the surface.

Another possible reason for the behavior of D near the surface could be the position of the evaporation front during drying. Wiberg[7] and Rosenkilde and Arfvidsson[4] show how the evaporation front recedes into the material in the capillary regime of drying, creating a dry "shell" near the surface. This dry shell probably exists also in the beginning of the diffusion regime. The dry shell may have caused $u_{i=1,j}$ to have lower values than they would have had if the dry shell had not existed. Hence, one can propose to include a dry shell formulation in future evaluations of D, as suggested by Salin.[12]

The calculations of D are sensitive to measurement errors of ρ_0, u, t, and x values, because derivatives of u in space and time are estimated by numerical schemes (Eqs. 8–11 and Eqs. 13–15). An error estimate of u based on the spread of the graph of $\dot{u}(t)$ calculated with a central difference approximation (Eq. 8) was made. The assumption was that $u(t)$ is a normally distributed stochastic variable and that t values are exact, which results in an estimated standard deviation of u of the order of 0.04% when u is approximately 20%. This standard deviation of u is considered low in comparison with earlier values (see Danvind[13]). It is believed that this spread in measured u values is the main cause of spread in D. The spread in D increases when u decreases.

Acknowledgments The authors express their gratitude to Valutec AB, Formas (the Swedish Research Council for Environment, Agricultural Sciences and Spatial Planning), Vinnova (the Swedish Agency for Innovation Systems) through the Skewood programme, and to Kempestiftelsen for their support.

References

1. Hukka A (1999) The effective diffusion coefficient and mass transfer coefficient of Nordic softwoods as calculated from direct drying experiments. Holzforschung 53:534–540
2. Hukka A, Oksanen O (1999) Convective mass transfer coefficient at wooden surface in jet drying of Veener. Holzforschung 53:204–208
3. Liu JY, Simpson WT, Verrill SP (2001) An inverse moisture diffusion algorithm for the determination of diffusion coefficient. Dry Technol 19:1555–1568
4. Rosenkilde A, Arfvidsson J (1997) Measurement and evaluation of moisture transport coefficients during drying of wood. Holzforschung 51:372–380
5. Lindgren O (1992) Medical CT-scanners for non-destructive wood density and MC measurements. Doctoral Thesis, Luleå University of Technology, Thesis No. 1992:111D
6. Danvind J, Morén T (2004) Using X-ray CT-scanning for moisture and displacement measurements in knots and their surroundings. EU COST 15 Wood Drying Conference Proceedings, April 22–23, Athens, Greece
7. Wiberg P (2001) X-ray CT-scanning of wood during drying. Doctoral Thesis, Luleå University of Technology, Thesis No. 2001:10
8. Ekevad M (2004) Method to compute fiber directions in wood from computed tomography images. J Wood Sci 50:41–46
9. Sepulveda P, Oja J, Grönlund A (2002) Predicting spiral grain by computed tomography of Norway spruce. J Wood Sci 48:479–483
10. Anon (2001) Matlab version 6.1.0.450 release 12.1. The MathWorks, Natick, MA
11. Anon (2003) ABAQUS users manual version 6.4. ABAQUS, Pawtucket, RI
12. Salin JG (2002) Theoretical analysis of mass transfer from wooden surfaces. Proceedings of 13th International Drying Symposium, 27–30 August, Beijing, China
13. Danvind J (2002) Measuring strain and moisture content in a cross-section of drying wood using digital speckle photography and computerised X-ray tomography. Proceedings of 13th International Symposium on Nondestructive Testing of Wood. 19–21 August, Berkley, CA, USA